


White matter integrity and key structures affected in Alzheimer's disease characterized by diffusion tensor imaging

Danqing Xiao^{1,2}  | Kesheng Wang³ | Luke Theriault^{1,4} | Elhelou Charbel¹ | Alzheimer's Disease Neuroimaging Initiative

¹Department of STEM, School of Arts and Sciences, Regis College, Weston, Massachusetts, USA

²Neuroimaging Center, McLean Hospital, Belmont, Massachusetts, USA

³Department of Family and Community Health, School of Nursing, Health Sciences Center, West Virginia University, Morgantown, West Virginia, USA

⁴School of Medicine, St. George's University, Saint George's, Grenada

Correspondence

Danqing Xiao, Department of STEM, School of Arts and Sciences, Regis College, Weston, MA 02493, USA.
Email: danqing.xiao@regiscollege.edu

Kesheng Wang, Department of Family and Community Health, School of Nursing, Health Sciences Center, West Virginia University, PO Box 9600, Office 6419, Morgantown, WV 26506, USA.
Email: kesheng.wang@hsc.wvu.edu

Abstract

White matter (WM) degeneration is suggested to predict the early signs of Alzheimer's disease (AD). The exact structural regions of brain circuitry involved are not known. This study aims to examine the associations between WM tract integrity, represented by the diffusion tensor imaging (DTI) measures, and AD diagnosis and to denote the key substrates in predicting AD. It included DTI measures of mean diffusivity (MD), fractional anisotropy, radial diffusivity and axial diffusivity of 18 main WM tracts in 84 non-Hispanic white participants from the Alzheimer's Disease Neuroimaging Initiative dataset. The multivariable general linear model was used to examine the association of AD diagnosis with each DTI measure adjusting for age, gender and education. The corpus callosum, fornix, cingulum hippocampus, uncinate fasciculus, sagittal striatum, left posterior thalamic radiation and fornix-stria terminalis showed significant increases in MD, radial and axial diffusivity, whereas the splenium of corpus callosum and the fornix showed significant decreases in fractional anisotropy among AD patients. Variable cluster analysis identified that hippocampus volume, mini-mental state examination (MMSE), cingulate

Abbreviations: ACR, anterior corona radiata; AD, Alzheimer's disease; ALIC, anterior limb of internal capsule; AxD, axial diffusivity; BCC, body of corpus callosum; CGC, cingulum (cingulate gyrus); CGH, cingulum hippocampus; CING/Hipp, cingulum/hippocampus; CN, cognitive normal control; CP, cerebral peduncle; CST, corticospinal tract; DTI, diffusion tensor imaging; EC, external capsule; FA, fractional anisotropy; FX, fornix (column and body); FX SUM, bilateral fornix sum; FX-ST, fornix (cres)-stria terminalis; GCC, genu of corpus callosum; HPV, hippocampus volume; IC, internal capsule; ICP, inferior cerebellar peduncle; IFO, inferior fronto-occipital fasciculus; ILF, inferior longitudinal fasciculus; _L, left side; MCI, mild cognitive impairment; MD, mean diffusivity; ML, medial lemniscus; MMSE, mini-mental state examination; PCR, posterior corona radiata; PLIC, posterior limb of internal capsule; PTR, posterior thalamic radiation including optic radiation; RLIC, retrolenticular part of internal capsule; _R, right side; RD, radial diffusivity; ROI, region of interest; SCC, splenium of corpus callosum; SCP, superior cerebellar peduncle; SCR, superior corona radiata; SFO, superior fronto-occipital fasciculus, SFO could be a part of AIC; SLF, superior longitudinal fasciculus; SS, sagittal stratum left and right includes ILF and IFO; SUMBCC, bilateral body of corpus callosum; SUMCC, bilateral full corpus callosum; SUMFX, bilateral fornix; SUMGCC, bilateral genu of corpus callosum; SUMSCC, bilateral splenium of corpus callosum; TAP, tapetum; Total CC, bilateral full corpus callosum average genu, body and splenium; UNC, uncinate fasciculus.

Data used in preparation of this article were obtained from the Alzheimer's Disease Neuroimaging Initiative (ADNI) database (adni.loni.usc.edu). As such, the investigators within the ADNI contributed to the design and implementation of ADNI and/or provided data but did not participate in analysis or writing of this report. A complete listing of ADNI investigators can be found at http://adni.loni.usc.edu/wp-content/uploads/how_to_apply/ADNI_Acknowledgement_List.pdf.

Present address

Luke Theriault, School of Medicine, St. George's University, Saint George's, Grenada.

Funding information

Regis College; DOD ADNI, Grant/Award Number: W81XWH-12-2-0012; Alzheimer's Disease Neuroimaging Initiative (ADNI), Grant/Award Number: U01 AG024904

Edited by: Anton Porsteinsson

gyrus/hippocampus, inferior fronto-occipital fasciculus and uncinate fasciculus are highly correlated in one cluster with MD measures. In conclusion, there were significant differences in DTI measures between the brain WM of AD patients and controls. Age is the risk factor associated with AD, not gender or education. Right cingulum gyms and right uncinate fasciculus are particularly affected, correlating well with a cognitive test MMSE and MD measures for dementia in AD patients and could be a region of focus for AD staging.

KEYWORDS

Alzheimer's disease, cingulate gyms, diffusion tensor imaging, hippocampus volume, mean diffusivity, mini-mental state examination, uncinate fasciculus

1 | INTRODUCTION

Alzheimer's disease (AD) is a common form of dementia—a syndrome that is marked by a severe decline in cognitive ability and which interferes with the ability to live independently. Depending on the level of cognitive impairment, AD can be differentiated into pre-clinical, mild cognitive impairment (MCI) and dementia stage (Kumar et al., 2021). AD and its clinical staging and mechanism have been studied extensively via its pathological findings of abnormal protein deposits, amyloid plaques and fibrillary tangles in the brain (e.g., Hyman et al., 2012; Jack et al., 2018). However, any degenerative changes in white matter (WM) tract that precede the loss of grey matter can occur years before the onset of symptoms (Araque Caballero et al., 2018; Nir et al., 2013; Wassenaar et al., 2018; Wen et al., 2018; Zhang et al., 2014). WM degeneration affecting myelination, myelin thickness, axon diameter and packing density is considered to predict AD in vivo and correlates with cerebrospinal fluid (CSF) biomarkers A β plaques (A β 42) and (phosphorylated-) Tau proteins (Araque Caballero et al., 2018; Bennett & Madden, 2014; Fjell et al., 2014; Hoy et al., 2017; Jack et al., 2018; Rieckmann et al., 2016; Strain et al., 2018; Wassenaar et al., 2018).

Functional magnetic resonance imaging (MRI) examining diffusion tensor imaging (DTI) measures has revealed microstructural WM differences between AD and control patients within the corpus callosum (CC), temporal lobe, frontal lobe and overall significant decreased connectivity within the default mode network (DMN) (Gao et al., 2020; Li et al., 2021; Mito et al., 2018; Sánchez et al., 2020), involving temporal WM starting in preclinical AD patients (Hoy et al., 2017; Mito et al., 2018; Nishioka et al., 2015; Weiler et al., 2017; Zhang et al., 2014). AD should be considered as a large-scale disconnection syndrome that may be associated with aggregation of toxic proteins and severe brain atrophy (Pereira et al., 2019). Fractional anisotropy

(FA) along with three other DTI measurable variables of diffusivity within DTI reflects fibre density, axonal diameter and myelination. The changes of these variables reflect changes in microstructure of the WM tract and provide a more sensitive biomarker for AD (Bennett & Madden, 2014; Daianu et al., 2013; Jack et al., 2018; Kantarci et al., 2017; Nir et al., 2013; Schaeffer et al., 2021; Sepehrband et al., 2019; Song et al., 2005; Wassenaar et al., 2018; Zhang et al., 2014). Mean diffusivity (MD) represents the average diffusion process in three directions (Wen et al., 2018). Loss of myelin results in the loss of fibre directionality, lower FA and higher MD, which are found in neurodegenerative diseases (Bennett & Madden, 2014; Kantarci et al., 2017; Nir et al., 2013), and also in individuals with increased genetic risk for AD (Rieckmann et al., 2016). MD correlated with other CSF markers, tau and amyloid protein (Araque Caballero et al., 2018; Nir et al., 2013), and is the most sensitive marker of the WM integrity among DTI measures, compared with measurements of volumetric reduction in identifying patients with MCI who will progress to AD (Araque Caballero et al., 2018; Fjell et al., 2014; Jack et al., 2018; Nir et al., 2015; Rieckmann et al., 2016; Wen et al., 2018; Zhang et al., 2014; Zhuang et al., 2013). The additional DTI measurements are axial diffusivity (AxD) in quantifying the diffusion parallel to axons and radial diffusivity (RD) reflecting the diffusions perpendicular to the axon (Alexander et al., 2007). AxD and RD changes have been shown to be markers for axonal damage and myelin damage, respectively (Bennett & Madden, 2014; Song et al., 2005). RD changes in AD have a similar trend as that seen with MD, which is the composite of AxD and RD (Rieckmann et al., 2016). Furthermore, MD and FA are associated with performance on clinical cognitive tests, such as the mini-mental state examination (MMSE) (Nir et al., 2015; Wen et al., 2018), with AD staging and with the presence of neurofibrillary tangles in the fornix (FX), cingulum tracts, entorhinal cortex and medial parietal cortex (Kantarci et al., 2017).

The analysis of the complete brain WM profile of all the available DTI data and its key components in AD compared with CN is incomplete. It is not known what specific WM regions are critical for triggering AD symptoms in patients with poor cognitive performance MMSE score and hippocampus atrophy. Further, limited studies on brain hemispheric asymmetry or lateralization in AD showed asymmetric neurodegeneration depending on the stages of AD and variability, and its link to pathogenesis and progression of AD is unclear (Lubben et al., 2021; Minkova et al., 2017). Additionally, the literature shows that age may have an impact on the pathogenesis of AD, whereas the impact of sex and education level is inconsistent (Fjell et al., 2014; Ribeiro et al., 2022). The present study examined the DTI measures of the WM tract throughout the brain WM tracts of AD patients and normal controls with use of data obtained from the Alzheimer's Disease Neuroimaging Initiative (ADNI) and any laterality of connectivity in the two hemispheres. Further, we examined the associations of age, gender and education with DTI measures. Lastly, we used variable cluster analysis to identify the most important structures among the major WM tracts that are affected in AD.

2 | MATERIALS AND METHODS

2.1 | The ADNI sample

Data used in the preparation of this article were obtained from the ADNI database (adni.loni.usc.edu). The ADNI, launched in 2003 led by Principal Investigator Michael W. Weiner, MD, is an ongoing, longitudinal, multicentre study designed to develop clinical, imaging, genetic and biochemical biomarkers for the early detection and tracking of AD. The primary goal of ADNI has been to test whether serial MRI, positron emission tomography (PET), other biological markers and clinical and neuropsychological assessment can be combined to measure the progression of MCI and early AD. The study was approved by Regis College's and West Virginia University's Institutional Review Boards.

2.2 | Image data acquisition and subject information

The DTI measurements (MD, FA, AxD and RD) and clinical data were downloaded from the ADNI database (www.loni.usc.edu/ADNI). DTI data of WM regions of interest (ROIs) were collected from the ADNI-2 and ADNI-3 project (see www.adni.org). DTI data were

generated from the Laboratory of NeuroImaging, University of South California (Nir et al., 2013). After merging DTI data with AD diagnosis, the present study used the baseline data from 84 non-Hispanic white participants ($n = 42$ for AD and $n = 42$ for healthy control CN). Demographic factors include gender (self-reported as either male or female), age and education (in years).

The MMSE was administered to provide a global measure of mental status, evaluating five cognitive domains: orientation, registration, attention and calculation, recall and language (Cockrell & Folstein, 1988). The MRI brain structure data were derived from UCSF FreeSurfer datasets. Hippocampus volume (HPV) was generated from UCSF MRI structure data.

2.2.1 | Brain regions

Briefly, the mean of all voxels from each of the WM tracts ROI from the atlas were obtained from maps of FA, MD, RD and AxD (Nir et al., 2013). In total, there are 228 ROI, including 18 main WM tract regions (CC, FX, CGH, CGC, UNC, IC, fronto-occipital fasciculus, EC, corona radiata, cerebellar peduncle, longitudinal fasciculus, SS, PTR, cerebral peduncle (CP), ML, FX-ST, TAP and CST). All available regions were used to derive comprehensive knowledge about the involvement of WM tract in AD. Processing methods for obtaining summary statistics in WM ROI include preprocessing steps and DTI maps, WM tract atlas ROI summary measures and tensor-based spatial statistics (TBSS) tract atlas ROI summary measures (adni.org). For TBSS tract atlas ROI summary measures, TBSS was performed, and the mean FA in ROI along the skeleton was extracted.

ROIs include the following in both hemispheres: corticospinal tract (CST), inferior cerebellar peduncle (ICP), superior cerebellar peduncle (SCP), CP, medial lemniscus (ML), anterior limb of internal capsule (ALIC), posterior limb of internal capsule (PLIC), posterior thalamic radiation (PTR, including optic radiation), anterior corona radiata (ACR), superior CR (SCR), posterior CR (PCR), cingulum/cingulate gyrus (CGC), cingulum hippocampus (CGH), superior longitudinal fasciculus (SLF), superior and inferior fronto-occipital fasciculus (SFO and IFO, respectively; SFO could be a part of AIC), sagittal stratum (SS) including inferior longitudinal fasciculus (ILF) and IFO, external capsule (EC), uncinata fasciculus (UNC), FX (column and body), genu of corpus callosum (GCC), body of corpus callosum (BCC), splenium of corpus callosum (SCC), retrolenticular part of internal capsule (RLIC), bilateral full corpus callosum average genu, body and splenium (total CC) and bilateral FX sum (FX sum). The left and right middle cerebellar peduncle and

pontine crossing tracts were excluded, as they often time fall partially or completely out of the field of view (FOV).

2.3 | Data analysis

Categorical variables were reported as count and continuous variables as mean \pm standard deviation (*SD*). The chi-square test was used to examine the association between gender and diagnosis. Male gender is considered as control and female gender is the treatment group. Student's *t* test was used to compare the means in age and education between CN and AD. Normality of DTI measures were tested by Kolmogorov–Smirnov statistics. For example, the *p* values of the statistics for MD_CGH left side and right side were .045 and .042, respectively, and skewness and kurtosis values in MD_CGH left side and right side were within (−3, 3), which indicated normal distributions and the general linear model (GLM) statistical analysis.

Multivariable GLM was used to examine the association of each DTI measure with AD diagnosis adjusting for age, gender and education. An *F* test in the GLM was used to test the overall model, while the *t* test in the GLM was used to detect the effect for each independent variable. Pearson and Spearman's rank correlation analyses were performed to explore the relationship among 31 MD measures, MMSE and HPV. Variable cluster analysis was used to examine multiple correlations among MD measures, MMSE and HPV, assuming strong correlation between variables in a cluster (Aggarwal, 2011; Muthen, 1985). A difference between groups with a *p* value $<.05$ was considered statistically significant. To deal with the multiple testing problem, Bonferroni correction was used for statistical significance. Considering

228 ROI, the Bonferroni corrected significant level will be a *p* value $<.05/228 = .00022$. All analyses were performed with SAS 9.4 (SAS Institute, Cary, North Carolina, USA).

2.4 | Statistical power analysis

We used G*Power v3.1.9.4 to compute the power for the present study (Faul et al., 2009, 2007). Based on the sample size ($n = 84$), given type 1 error rate ($\alpha = .05$), moderate effect size (.15), using *F* test in multivariable linear regression model with four predictors (AD diagnosis and three demographic factors—age, gender and education), the power could reach 79.74%.

3 | RESULTS

3.1 | Descriptive statistics

There was no significant difference in age or gender between AD and normal control group (Table 1). The CN group had a significantly greater education level than the AD group ($p = .0437$). Furthermore, CN individuals had significantly higher values in MMSE and HPV than the AD individuals (both *p* values $<.0001$).

3.2 | GLM analysis of diagnosis of AD with DTI measures

Table 2 presents the results based on multivariable GLM analysis of AD with DTI measures ($p < .01$), where *p* values smaller than .00022 (indicated with a ‘*’) show

TABLE 1 Descriptive statistics

Variable	CN	AD	χ^2/t value	<i>p</i>
Gender				
Male	19	25	1.71	.1899
Female	23	17		
Age				
Mean \pm <i>SD</i>	72.74 \pm 5.82	74.44 \pm 8.61	1.06	.2936
Education				
Mean \pm <i>SD</i>	16.36 \pm 2.77	15.14 \pm 2.66	−2.05	.0437
MMSE				
Mean \pm <i>SD</i>	28.88 \pm 1.40	23.36 \pm 1.85	−15.45	<.0001
HPV				
Mean \pm <i>SD</i>	7484.54 \pm 924.83	5930.72 \pm 800.65	−7.58	<.0001

Note: *p* value is based on chi-square or *t* test.

Abbreviations: AD, Alzheimer's disease; CN, cognitive normal; HPV, hippocampus volume (in mm³); MMSE, mini-mental state examination.

TABLE 2 Multivariable linear regression analyses of DTI measures with Alzheimer's disease diagnosis (AD vs. CN)

Brain regions	MD (β , t , p)	FA (β , t , p)	AxD (β , t , p)	RD (β , t , p)
SUMGCC	.0114, 4.08, <.0001*	-3.1232, -2.42, .0180	.0109, 4.38, <.0001*	.0116, 3.67, .0004*
SUMBCC	.0142, 4.86, <.0001*	-2.9070, -2.66, .0095	.0137, 5.30, <.0001*	.0144, 4.51, <.0001*
SUMSCC	.0136, 5.08, <.0001*	-4.2449, -4.21, <.0001*	.0128, 4.99, <.0001*	.0140, 4.97, <.0001*
SUMCC	.0139, 5.23, <.0001*	-3.7714, -3.60, .0006	.0131, 5.57, <.0001*	.0143, 4.93, <.0001*
GCC_L	.0121, 4.40, <.0001*	-3.3530, -2.66, .0093	.0116, 4.73, <.0001*	.0124, 3.97, .0002*
GCC_R	.0106, 3.64, .0005	-2.9018, -2.12, .0368	.0103, 3.74, .0004	.0108, 3.31, .0014
BCC_L	.0149, 4.92, <.0001*	-2.8212, -2.47, .0156	.0151, 5.53, <.0001*	.0147, 4.46, <.0001*
BCC_R	.0135, 4.51, <.0001*	-2.9967, -2.78, .0067	.0123, 4.48, <.0001*	.0141, 4.35, <.0001*
SCC_L	.0167, 5.13, <.0001*	-4.6943, -4.33, <.0001*	.0161, 5.14, <.0001*	.0169, 4.99, <.0001*
SCC_R	.0108, 4.66, <.0001*	-3.8299, -3.91, .0002*	.0097, 4.26, <.0001*	.0113, 4.64, <.0001*
SUMFX	.0344, 5.84, <.0001*	-4.7488, -5.39, <.0001*	.0286, 5.46, <.0001*	.0373, 5.86, <.0001*
FX_L	.0411, 5.63, <.0001*	-5.3806, -5.07, <.0001*	.0330, 4.91, <.0001*	.0451, 5.75, <.0001*
FX-R	.0326, 5.42, <.0001*	-4.6292, -4.78, <.0001*	.0276, 5.26, <.0001*	.0351, 5.36, <.0001*
CGH_L	.0161, 7.98, <.0001*	-1.9223, -3.57, .0006	.0169, 7.87, <.0001*	.0157, 7.85, <.0001*
CGH_R	.0110, 4.87, <.0001*	-1.5440, -2.49, .0150	.0117, 5.24, <.0001*	.0107, 4.59, <.0001*
CGC_L	.0046, 3.91, .0002*	-.7954, -1.39, .1695	.0043, 3.57, .0006	.0047, 3.79, .0003
CGC_R	.0041, 3.45, .0009	-.7308, -1.22, .2255	.0039, 3.54, .0007	.0041, 3.21, .0019
UNC_L	.0234, 6.64, <.0001*	-1.2464, -1.64, .1047	.0253, 6.90, <.0001*	.0225, 6.40, <.0001*
UNC_R	.0180, 5.22, <.0001*	-2.1234, -3.19, .002	.0184, 5.11, <.0001*	.0178, 5.22, <.0001*
SFO_L	.0253, 3.48, .0008	-1.4879, -1.61, .1118	.0262, 3.48, .0008	.0249, 3.47, .0009
SFO_R	.0223, 3.92, .0002*	-3.0704, -3.68, .0004	.0211, 3.56, .0006	.0229, 4.09, .0001*
IFO_L	.0068, 4.37, <.0001*	-1.5484, -2.24, .028	.0067, 3.69, .0004	.0068, 4.35, <.0001*
IFO_R	.0061, 3.15, .0023	-1.1930, -1.69, .0959	.0063, 3.14, .0024	.0061, 3.02, .0034
SCR_L	.0065, 4.29, <.0001*	1.2004, 1.75, .0846	.0099, 5.00, <.0001*	.0048, 3.50, .0008
SCR_R	.0065, 3.72, .0004	.9459, 1.36, .1765	.0094, 4.29, <.0001*	.0051, 3.16, .0022
ACR_L	.0062, 3.69, .0004	-1.8846, -3.10, .0027	.0053, 2.91, .0047	.0066, 3.95, .0002*
ACR_R	.0069, 3.80, .0003	-1.6291, -2.36, .0205	.0064, 3.43, .001	.0071, 3.81, .0003
SS_L	.0112, 7.26, <.0001*	-1.5279, -2.67, .0091	.0140, 7.05, <.0001*	.0114, 7.02, <.0001*
SS_R	.0121, 5.49, <.0001*	-1.1267, -1.95, .0553	.0138, 5.56, <.0001*	.0113, 5.27, <.0001*
PTR_L	.0105, 4.11, <.0001*	-2.0307, -2.53, .0135	.0108, 4.15, <.0001*	.0103, 3.98, .0002*
PTR_R	.0061, 3.04, .0032	-1.5791, -2.19, .0314	.0060, 2.81, .0062	.0061, 3.04, .0032

Note: t and p values are based on multivariable linear regression analyses of DTI measures in comparison with Alzheimer's disease with cognitive normal. β is regression coefficient * 100.

Abbreviations: ACR, anterior corona radiata; AxD, axial diffusivity; BCC, body of corpus callosum; CGC, cingulate gyrus; CGH, cingulum hippocampus; FA, fractional anisotropy; FX, fornix (column and body); GCC, genu of corpus callosum; IFO, inferior fronto-occipital fasciculus; L, left; MD, mean diffusivity; PTR, posterior thalamic radiation; R, right; RD, radial diffusivity; SCC, splenium of corpus callosum; SCR, superior corona radiata; SFO, superior fronto-occipital fasciculus; SS, sagittal stratum; SUMBCC, bilateral body of corpus callosum; SUMCC, bilateral full corpus callosum; SUMFX, bilateral fornix; SUMGCC, bilateral genu of corpus callosum; SUMSCC, bilateral splenium of corpus callosum; UNC, uncinata fasciculus.

* $p < .00022$.

statistical significance based on Bonferroni correction. A comprehensive list of DTI measures in all 228 ROI regions is presented in Table S1. Overall, compared with CN, AD showed significant higher values in MD, RD and AxD measures, but lower FA values in some specific ROI regions (Table 2).

AD individuals had significantly higher MD values in SUMCC, FX, FX-ST, CGH, PTR_L, SCR_L, SS, IFO_L/SFO_R, UNC and tapetum (TAP) (fibre of the body and splenium of CC), compared with healthy controls (Tables 2 and S1). Significance of AxD changes (diffusion parallel to the axon, marker for axonal damage) is similar

(to MD values) for the most ROIs, except, CGC_L and IFO_L and SFO_R, but gained significance in SCR_R, in comparison with healthy CN controls. On the other hand, the significance of RD values changes (for diffusion perpendicular to the axon, marker for myelin damage) is similar (to MD values) for the most ROIs, except in CGC_L, but gained significance in ACR_L, in comparison with healthy CN controls. In contrast, AD individuals had significantly lower FA values in both hemispheres, measured independently, in SCC, FX and FX-ST only.

The significance of changes in the four DTI measures showed leftward brain asymmetry among the ROIs (Tables 2 and S1). In this asymmetry, the left side of brain had more ROIs, WM tract regions, showed significant changes of DTI measures (not the right side). For MD, these WM tracts included GCC, CGC, IFO, SCR and PTR. For RD, these WM tracts included GCC, IFO, ACR, PTR and TAP. In AxD, these WM tracts ROIs included GCC, PTR, RLIC and PCR. For FA, these WM tracts included TAP only.

However, only SFO WM region showed significant increases in MD and RD values in the right side (not the left side).

3.3 | Associations of age, gender and education with DTI measures

The results of associations of age, gender and education with DTI measures based on the multivariable GLM analyses on all 84 subjects are presented in Table S2A–D. Age is significantly associated with the increased diffusivity (MD, RD and AxD) and reduced FA in certain ROIs. Specifically, the increased diffusivity MD and RD was found in ROIs of GCC, CGH, RLIC, EC_L, SCR_L, SS_L, FX-ST_L and CST_R (with additional ROIs of ALIC and ACR having increased RD values), and increased AxD in SS_L, FX-ST_L and CST_R, but decreased FA in overlapping ROIs in CGH_R, RLIC_R, EC_L, ACR, ICP, ML_L and FX-ST_L.

Regarding gender and education, although gender and education were associated with certain DTI measures at p values $<.05$, after corrections for multiple comparisons, gender and education did not have significant impact on all the four DTI measures (Table S2A–D).

3.4 | Correlational and cluster analysis

Correlational and variable cluster analysis was conducted on 31 MD measures, MMSE and HPV in both AD and CN groups (all p values $<.0001$). These variables were grouped into four clusters with strong relationships

among variables within each cluster (Figure 1). CGC, CGH, IFO, UNC measures, MMSE and HPV had strong significant correlations and were grouped within a cluster, while Pearson and Spearman correlation coefficients are presented in Table 3. MMSE and HPV showed significant positive correlations, while MD measures showed significant positive correlations (between the left and the right side of the same WM and among the eight ROIs). However, MMSE and HPV showed strong negative correlations with MD measures of all eight ROI regions. In other words, individuals with higher MMSE and HPV values had lower MD measures.

The AD group had higher mean values of MD in CGC, CGH, IFO, UNC measures than in CN group (Figure 2). In addition, variable cluster analyses were performed for AD and CN, separately (Figures 3 and 4). In the CN group, CGH, IFO, UNC measures, MMSE and HPV had strong correlations and were grouped within a cluster, whereas CGC measures were clustered in another flanking cluster (Figure 4). Among the AD group, CGC_R, CGH, IFO, UNC_R measures, MMSE and HPV had strong correlations and were grouped within a cluster, whereas CGC_L and UNC_L were clustered in another flanking cluster (Figure 3). In other words, right CGC and UNC are uniquely affected in the AD, not in the CN group. Further, In CN, MMSE cluster is close to PTR, SCR, CGC and SS group. In AD, MMSE cluster is close to a group with different brain WM tract regions, ACR, SCR, SFO, UNC-L and CC, suggesting the connectivity underlying MMSE in link to HPV is altered in AD.

4 | DISCUSSION

The present study comprehensively mapped all the major WM tracts in AD compared with CN, including both hemispheres using all four DTI measures, their association with age, gender and education using the ADNI data. Additionally, we pinpointed the key structures linked to cognitive performance and hippocampal volume underlying AD using clusters analysis. Significant associations with DTI measures were found in WM tracts connecting frontal, parietal, temporal and occipital lobes, suggesting the myelination and axonal integrity have been damaged. By using a larger AD population sample than previous one (e.g., Nir et al., 2013), we showed the complete profile of significant changes (increased diffusivity and reduced FA) in all the four DTI measures in ROIs of SCC, FX, FX-ST and TAP_L, with increased diffusivity of MD, RD, AxD in additional WM tracts, SUMCC, CGH, PTR_L, UNC and SS. The present study found that the CST is spared. The changes explain the cardinal signs of disturbance in limbic functions

(memory and emotion) in AD patients. Motor disturbance could appear in more advanced states of AD. Among age, gender and education, age has significant association with DTI measures, increased diffusivity and reduced anisotropy FA. Gender and education level

has no association with these DTI measures. Finally, CGC, CGH, IFO and UNC are significantly correlated with MMSE and hippocampal volumes among all the examined WM tracts. Right CGC and right UNC are uniquely correlated in AD, not in CN.

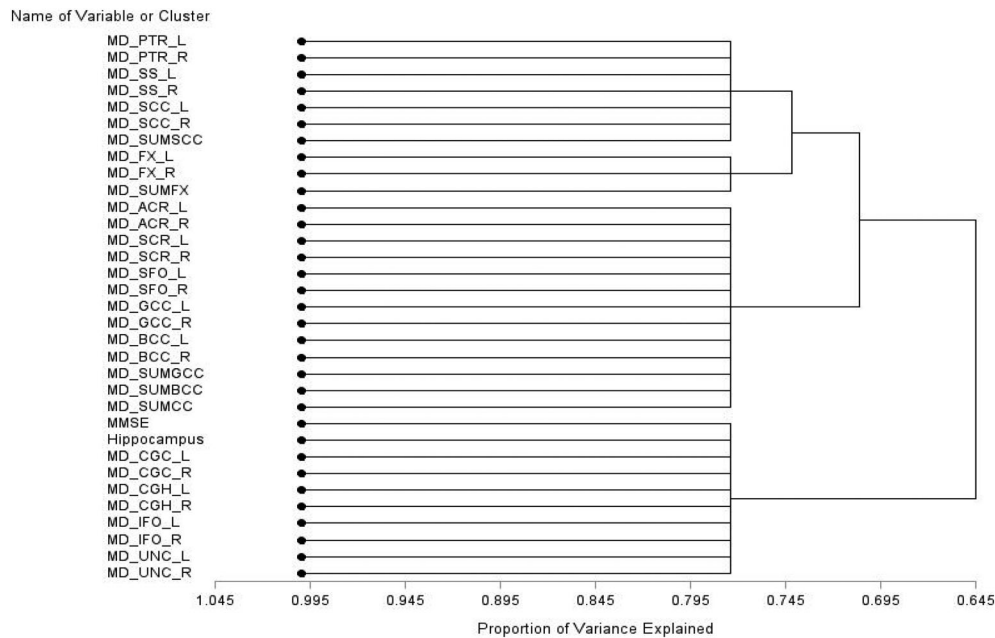


FIGURE 1 Variable cluster analysis of MD measures and MMSE and hippocampus for both AD and CN ($n = 84$). MD refers to mean diffusivity; MMSE refers to mini-mental state examination. These variables were grouped into four clusters with strong relationships among variables in each cluster. MMSE had strong correlations with CGC, CGH, IFO, UNC measures and hippocampus volume and were grouped within a cluster. Abbreviations for the brain regions: SUMGCC, bilateral genu of corpus callosum; SUMBCC, bilateral body of corpus callosum; SUMSCC, bilateral splenium of corpus callosum; SUMCC, bilateral full corpus callosum; GCC, genu of corpus callosum; BCC, body of corpus callosum; SCC, splenium of corpus callosum; SUMFX, bilateral fornix; FX, fornix (column and body); CGH, cingulum hippocampus; CGC, cingulate gyrus; UNC, uncinate fasciculus; SFO, superior fronto-occipital fasciculus; IFO, inferior fronto-occipital fasciculus; SCR, superior corona radiata; ACR, anterior corona radiata; SS, sagittal stratum; PTR, posterior thalamic radiation

TABLE 3 Correlation analysis of MD measures and MMSE and HPV ($n = 84$)

Variable	MMSE	HPV	CGC_L	CGC_R	CGH_L
MMSE	1	.6455 < .0001	-.5151 < .0001	-.4539 < .0001	-.6157 < .0001
HPV	.6731 < .0001	1	-.4808 (r) < .0001 (p)	-.5163 < .0001	-.7259 < .0001
CGC_L	-.5236 < .0001	-.5098 < .0001	1	.8014 < .0001	.6201 < .0001
CGC_R	-.5006 < .0001	-.5357 < .0001	.8417 < .0001	1	.5948 < .0001
CGH_L	-.6320 < .0001	-.7900 < .0001	.6625 < .0001	.6086 < .0001	1
CGH_R	-.5752 < .0001	-.7715 < .0001	.5958 < .0001	.5967 < .0001	.7028 < .0001
IFO_L	-.4922 < .0001	-.5919 < .0001	.7218 < .0001	.7394 < .0001	.6659 < .0001
IFO_R	-.4776 < .0001	-.6269 < .0001	.7621 < .0001	.7693 < .0001	.6341 < .0001
UNC_L	-.5716 < .0001	-.6453 < .0001	.6096 < .0001	.5999 < .0001	.7234 < .0001
UNC_R	-.5870 < .0001	-.6524 < .0001	.6075 < .0001	.6412 < .0001	.6312 < .0001

Note: Above the diagonal is the Pearson correlation coefficient; below the diagonal is Spearman correlation coefficient. Lower value in each cell denotes the p value.

Abbreviations: CGC, cingulate gyrus; CGH, cingulum hippocampus; HPV, hippocampus volume (in mm^3); IFO, inferior fronto-occipital fasciculus; L, left; MD, mean diffusivity; MMSE, mini-mental state examination; R, right; UNC, uncinate fasciculus.

TABLE 3 (Continued)

Variable	CHG_R	IFO_L	IFO_R	UNC_L	UNC_R
MMSE	-.4901 < .0001	-.5030 < .0001	-.3660 < .0006	-.5400 < .0001	-.5124 < .0001
HPV	-.7007 < .0001	-.5624 < .0001	-.5813 < .0001	-.5629 < .0001	-.6114 < .0001
CGC_L	.4872 < .0001	.6902 < .0001	.6025 < .0001	.5757 < .0001	.4908 < .0001
CGC_R	.5383 < .0001	.7100 < .0001	.6904 < .0001	.5517 < .0001	.5803 < .0001
CGH_L	.5894 < .0001	.6964 < .0001	.5420 < .0001	.6229 < .0001	.5201 < .0001
CGH_R	1	.5476 < .0001	.6615 < .0001	.5643 < .0001	.7480 < .0001
IFO_L	.6253 < .0001	1	.7233 < .0001	.5951 < .0001	.4171 < .0001
IFO_R	.6704 < .0001	.8038 < .0001	1	.6087 < .0001	.6157 < .0001
UNC_L	.6494 < .0001	.6355 < .0001	.6510 < .0001	1	.6206 < .0001
UNC_R	.7502 < .0001	.5113 < .0001	.6917 < .0001	.6453 < .0001	1

Note: Above the diagonal is the Pearson correlation coefficient; below the diagonal is Spearman correlation coefficient. Lower value in each cell denotes the *p* value.

Abbreviations: CGC, cingulate gyrus; CGH, cingulum hippocampus; HPV, hippocampus volume (in mm³); IFO, inferior fronto-occipital fasciculus; L, left; MD, mean diffusivity; MMSE, mini-mental state examination; R, right; UNC, uncinata fasciculus.

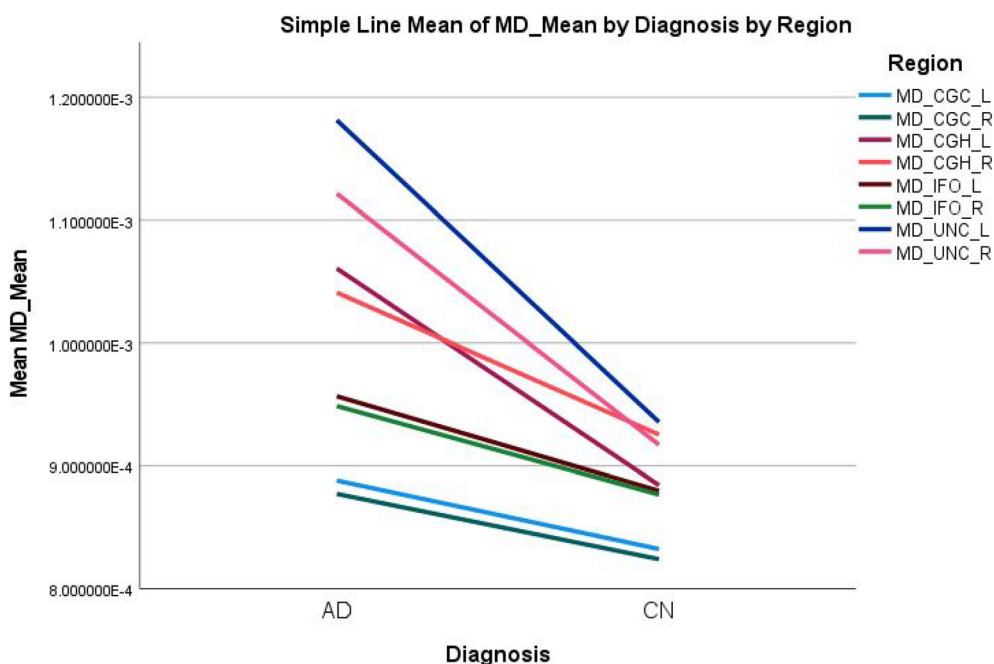


FIGURE 2 Mean values of MD measures in AD and CN groups. MD refers to mean diffusivity, CN refers to cognitive normal, and AD refers to Alzheimer’s disease. Abbreviations for the brain regions: CGH, cingulum hippocampus; CGC, cingulate gyrus; UNC, uncinata fasciculus; IFO, inferior fronto-occipital fasciculus

Circuitries for memory, emotion and senses underlying AD are affected differently. First, studies have shown that changes in circuitry for memory and emotion underlie AD, including the DMN network for episodic memory involving medial entorhinal, medial orbitofrontal and lateral frontal, precuneus, middle temporal hippocampus and inferior parietal cortex (Aggleton et al., 2016; Bigham et al., 2020; Fjell et al., 2014). The present study identified that MD changes existed in these regions, overlapping with DMN including the cingulum, hippocampus and FX and other WM tracts connecting the brain lobes. Specifically, our cluster analysis identified that hippocampus,

cingulate gyrus/hippocampus (CGC and CGH), IFO and UNC are highly correlated in one cluster with MD changes associated with MMSE cognitive phenotypes for both AD and CN, providing a more specific model than previously proposed (Qin et al., 2021). Furthermore, our findings of changes in the PTR support previous results suggesting that thalamic pathology is implicated in the early stage of AD contributing to emotional disturbance (Wen et al., 2018). Especially, our finding of age being significantly associated with MD changes in FX-ST (not FX) suggested that aging significantly affects emotional processing (see Figure S2A). Lastly, FA reduction

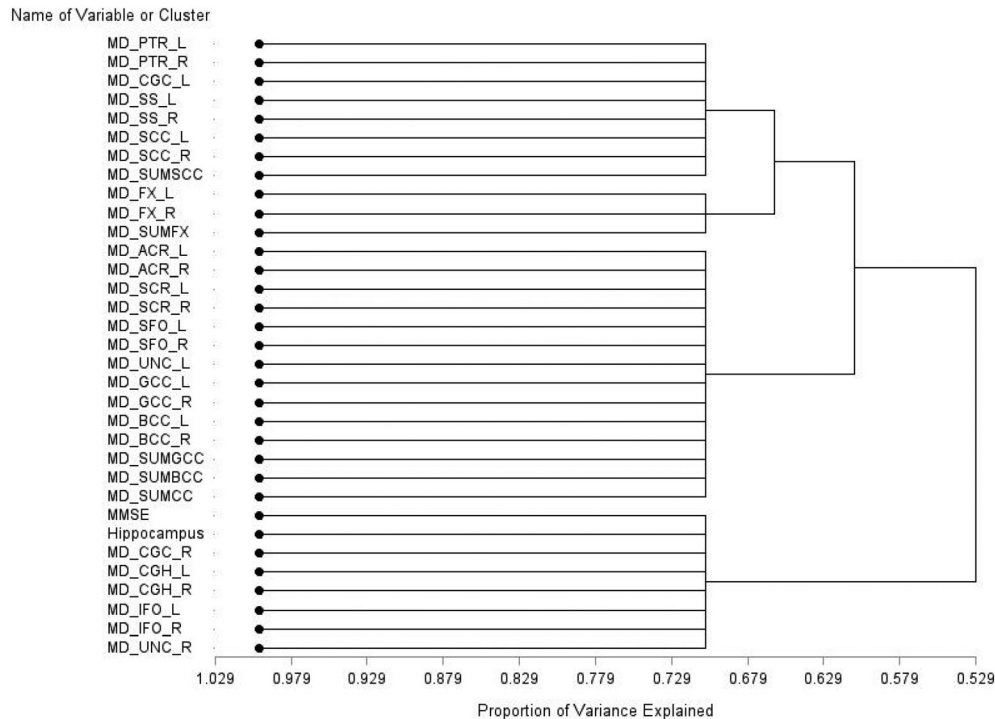


FIGURE 3 Variable cluster analysis of MD measures and MMSE and hippocampus (volume) in AD ($n = 42$). MD refers to mean diffusivity; MMSE refers to mini-mental state examination. These variables were grouped into four clusters with strong relationships among variables in each cluster. MMSE had strong correlations with CGC, CGH, IFO, UNC measures and hippocampus volume and were grouped within a cluster. Abbreviations for the brain regions: SUMGCC, bilateral genu of corpus callosum; SUMBCC, bilateral body of corpus callosum; SUMSCC, bilateral splenium of corpus callosum; SUMCC, bilateral full corpus callosum; GCC, genu of corpus callosum; BCC, body of corpus callosum; SCC, splenium of corpus callosum; SUMFX, bilateral fornix; FX, fornix (column and body); CGH, cingulum hippocampus; CGC, cingulate gyrus; UNC, uncinate fasciculus; SFO, superior fronto-occipital fasciculus; IFO, inferior fronto-occipital fasciculus; SCR, superior corona radiata; ACR, anterior corona radiata; SS, sagittal stratum; PTR, posterior thalamic radiation

in the regions of SCC, and TAP might explain the visual disturbance and other loss of special senses in MCI and AD patients (Nishioka et al., 2015; Wassenaar et al., 2018). Primary somatosensory and motor areas are least affected at least at the early stage of AD.

Previous studies have shown that a breakdown in connectivity occurs during the aging process in normal individuals with gradual decline of FA and increased MD and RD (Bennett & Madden, 2014; Zhuang et al., 2013) and in the early stage of AD (Zhang et al., 2014). Our results showed that this breakdown is particularly exacerbated in the left side of the brain with more ROIs involved, that is, brain asymmetry. Indeed, we found a more significant impact of age on DTI values than gender and education. This is consistent with what we know about aging being a contributing factor (correlating with cortical thinness) towards the development of AD, with annual atrophy of entorhinal cortex, progressing to the parietal, frontal regions and ultimately to all regions of cortex (Fjell et al., 2014). It is hypothesized that the limbic area is the most vulnerable due to the demand of neuroplasticity in the face of lesion and other injury insults.

In contrast to normal aging, the AD processes lead to greater impact on tempo-parietal cortex, including entorhinal cortex, hippocampus, posterior cingulate and retrosplenial cortex, which is involved in episodic memory (Fjell et al., 2014). The present study did not find significant differences in DTI measures between genders, consistent with previous findings (Wu et al., 2011) and in mild cognitive impaired participant (O'Dwyer et al., 2012). We did not find that education has any significant effect on DTI measures either. Similarly, previous findings have shown that the effect of education or intellectual activities on brain biomarkers such as amyloid deposition is ambiguous (Fjell et al., 2014).

We found a significant MD increase in CC, FX, cingulum, UNC, SFO and IFO, SCR, sagittal striatum and thalamic radiation, the areas that are vulnerable for modifiable risk factors for AD (Wassenaar et al., 2018). Importantly, our study used cluster analysis and pinpointed the key WM structural changes in the brain connectivity in AD associated with cognitive test MMSE and hippocampal volume changes. These six ROIs are right CGC, bilateral hippocampal cingulum, bilateral IFO and

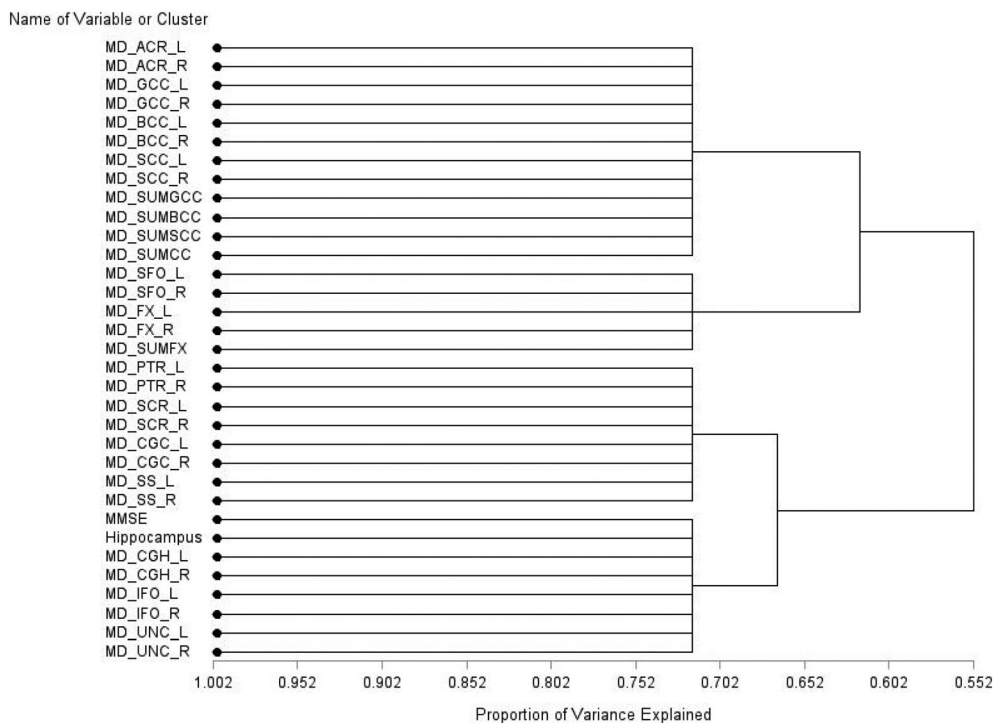


FIGURE 4 Variable cluster analysis of MD measures and MMSE and hippocampus (volume) in CN ($n = 42$). MD refers to mean diffusivity; MMSE refers to mini-mental state examination. These variables were grouped into four clusters with strong relationships among variables in each cluster. MMSE had strong correlations with CGC, CGH, IFO, UNC measures and hippocampus volume and were grouped within a cluster. Abbreviations for the brain regions: SUMGCC, bilateral genu of corpus callosum; SUMBCC, bilateral body of corpus callosum; SUMSCC, bilateral splenium of corpus callosum; SUMCC, bilateral full corpus callosum; GCC, genu of corpus callosum; BCC, body of corpus callosum; SCC, splenium of corpus callosum; SUMFX, bilateral fornix; FX, fornix (column and body); CGH, cingulum hippocampus; CGC, cingulate gyrus; UNC, uncinate fasciculus; SFO, superior fronto-occipital fasciculus; IFO, inferior fronto-occipital fasciculus; SCR, superior corona radiata; ACR, anterior corona radiata; SS, sagittal stratum; PTR, posterior thalamic radiation

right UNC which are worthwhile to be studied further in depth. Among the above regions, changes in the right CGC and right UNC are unique to AD patients, not in CN. UNC is subjacent to IFO, connecting frontal and temporal cortex, its function is not well defined. The right CGC is correlated with smell loss in COVID-19 patients (Lu et al., 2020). The loss of the connection with right CGC and uncinate might explain the loss of smell, a very early symptom of AD. Compared with a previous study (e.g., Nir et al., 2013), we were able to narrow down the key structures to right CGC and right UNC, that is responsible for the declined cognitive performance MMSE scores in AD. Studying the pattern of changes in brain regions will help to elucidate what triggers the switch to AD disease progression, for example, accelerated atrophy in the temporal cortex, the cingulate and orbitofrontal cortex (Fjell et al., 2014). AD starts with subtle cognitive changes identified over 10 years before the onset of dementia. Our study suggests that right CGC and right UNC could be such a trigger switch to AD; then, the disconnectivity spreads to the left side of the brain regions leading to impairment in language skills.

Finally, further identification and characterization of the specific WM degeneration and synaptic loss within AD may help distinguish its neuropathology from other forms of dementia such as Lewy body disease. A thorough examination of the nature and location of WM degeneration within AD may help with the staging of AD and in early diagnosis.

This study has several strengths. First, we compared the DTI measures between AD and CN using multivariable linear regression model and adjusted for age, gender and education. Second, we performed variable cluster analysis of MD measures and MMSE and HPV. In addition, the present study also examined the effects of age, gender and education on the DTI measures. We acknowledge some limitations. First, the sample size is relatively small although the use of multivariable linear regression analysis could achieve power close to 80%. Second, to reduce ethnic heterogeneity, this study just used non-Hispanic white individuals; therefore, the results limit the generalizability of the findings to explore effects both within and across the groups for non-White populations (African American and Hispanic). Further work that

concentrates on people of different ethnic/racial backgrounds is needed. Third, this study focused on comparison of AD with CN. In the future, it will be interesting to further compare DTI measures of MCI with CN.

Our study suggests that the functions of WM tracts, CGC, hippocampal cingulum, long associative fibre tract IFO and the short UNC play important roles in cognitive memory test MMSE. In particular, breakdown of right CGC and right UNC in AD links to poor MMSE performance and atrophy of hippocampal volume. Among the structures studied, the DTI measure of these two structures (CGC-R and UNC-R) might provide a sensitive early biomarker for Alzheimer's disease.

5 | CONCLUSION

In summary, our findings support the use of DTI measures for early detection of the onset of AD, in particular, the right CGC and the right UNC should be the WM tracts of focus, based on cluster analysis. Second, this research supported the view that the WM disconnectivity and brain asymmetry being the source of pathogenesis in AD. Among the WM tracts, the CC (including TAP), FX, CGH, UNC, sagittal striatum, left PTR and fornix-stria terminalis showed significant increases in diffusivity, whereas only splenium of CC and FX showed significant decreases in FA among AD patients. Finally, aging is the main risk factor associated with the change of these DTI measures in AD, not gender or education level.

Significant correlations were found among DTI measures in MD, outcomes of MMSE and HPV. Increased MD in right CGC and right UNC correlated to a poor cognitive memory task performance in AD but not in CN. This detailed study of individual brain WM tracts supported that DTI measures (especially MD) in CGC and UNC (right side) can be a sensitive biomarker in predicting, clinical staging and monitoring treatment of AD.

ACKNOWLEDGEMENTS

The present study is a secondary data analysis. The original study and ADNI was funded by the Alzheimer's Disease Neuroimaging Initiative (ADNI) (National Institutes of Health Grant U01 AG024904) and DOD ADNI (Department of Defense award number W81XWH-12-2-0012). ADNI is funded by the National Institute on Aging, the National Institute of Biomedical Imaging and Bioengineering and through generous contributions from the following: AbbVie, Alzheimer's Association; Alzheimer's Drug Discovery Foundation; Araclon Biotech; BioClinica, Inc.; Biogen; Bristol-Myers Squibb Company; CereSpir, Inc.; Cogstate; Eisai Inc.; Elan Pharmaceuticals, Inc.; Eli Lilly and Company;

EuroImmun; F. Hoffmann-La Roche Ltd and its affiliated company Genentech, Inc.; Fujirebio; GE Healthcare; IXICO Ltd.; Janssen Alzheimer Immunotherapy Research & Development, LLC.; Johnson & Johnson Pharmaceutical Research & Development LLC.; Lumosity; Lundbeck; Merck & Co., Inc.; Meso Scale Diagnostics, LLC.; NeuroRx Research; Neurotrack Technologies; Novartis Pharmaceuticals Corporation; Pfizer Inc.; Piramal Imaging; Servier; Takeda Pharmaceutical Company; and Transition Therapeutics. The Canadian Institutes of Health Research is providing funds to support ADNI clinical sites in Canada. Private sector contributions are facilitated by the Foundation for the National Institutes of Health (www.fnih.org). The grantee organization is the Northern California Institute for Research and Education, and the study is coordinated by the Alzheimer's Therapeutic Research Institute at the University of Southern California. ADNI data are disseminated by the Laboratory for NeuroImaging at the University of Southern California. The authors would like to thank the support of Kaneb Grant 2020–2022 from Regis College, Dr. Lisa Glickstein (Regis College, Weston, MA) and Dr. David Kindelberger (Atrius Health, Needham, MA) for comments and editing on the manuscript.

CONFLICT OF INTEREST

All authors have reported no financial interests or potential conflicts of interest.

AUTHOR CONTRIBUTIONS

DX is involved in conceptualization, investigation, supervision, project administration and funding acquisition. DX and LT searched for literature and conducted literature review. DX, KW and LT contributed to data management and statistical analysis and drafted part of the manuscript. EC contributed to tables. All authors were involved in a substantive review of the manuscript. All authors read and approved the manuscript.

PEER REVIEW

The peer review history for this article is available at <https://publons.com/publon/10.1111/ejn.15815>.

DATA AVAILABILITY STATEMENT

The data were downloaded from the Alzheimer's Disease Neuroimaging Initiative (ADNI) database (<http://adni.loni.usc.edu/>). Application for access to the ADNI data can be submitted by anyone at <http://adni.loni.usc.edu/data-samples/access-data/>. The process includes completion of an online application form and acceptance of Data Use Agreement. All data used in the study were downloaded from ADNI in May 2020.

ORCID

Danqing Xiao  <https://orcid.org/0000-0002-6963-2933>

REFERENCES

- Aggarwal, V. K. S. (2011). *Feather selection and dimension reduction techniques in SAS*. NESUG.
- Aggleton, J. P., Pralus, A., Nelson, A. J., & Hornberger, M. (2016). Thalamic pathology and memory loss in early Alzheimer's disease: Moving the focus from the medial temporal lobe to Papez circuit. *Brain*, *139*(Pt 7), 1877–1990. <https://doi.org/10.1093/brain/aww083>
- Alexander, A. L., Lee, J. E., Lazar, M., & Field, A. S. (2007). Diffusion tensor imaging of the brain. *Neurotherapeutics*, *4*(3), 316–329. <https://doi.org/10.1016/j.nurt.2007.05.011>
- Araque Caballero, M. Á., Suárez-Calvet, M., Duering, M., Franzmeier, N., Benzinger, T., Fagan, A. M., Bateman, R. J., Jack, C. R., Levin, J., Dichgans, M., Jucker, M., Karch, C., Masters, C. L., Morris, J. C., Weiner, M., Weiner, M., Rossor, M., Fox, N. C., Lee, J. H., ... Ewers, M. (2018). White matter diffusion alterations precede symptom onset in autosomal dominant Alzheimer's disease. *Brain*, *141*(10), 3065–3080. <https://doi.org/10.1093/brain/awy229>
- Bennett, I. J., & Madden, D. J. (2014). Disconnected aging: Cerebral white matter integrity and age-related differences in cognition. *Neuroscience*, *276*, 187–205. <https://doi.org/10.1016/j.neuroscience.2013.11.026>
- Bigham, B., Zamanpour, S. A., Zemorshidi, F., Boroumand, F., & Zare, H. (2020). Identification of superficial white matter abnormalities in Alzheimer's disease and mild cognitive impairment using diffusion tensor imaging. *Journal of Alzheimer's Disease Reports*, *4*(1), 49–59. <https://doi.org/10.3233/adr-190149>
- Cockrell, J. R., & Folstein, M. F. (1988). Mini-Mental State Examination (MMSE). *Psychopharmacology Bulletin*, *24*(4), 689–692.
- Daianu, M., Dennis, E. L., Jahanshad, N., Nir, T. M., Toga, A. W., Jack, C. R. Jr., Weiner, M. W., & Thompson, P. M. (2013). Alzheimer's disease disrupts rich club organization in brain connectivity networks. In *2013 IEEE 10th International Symposium on Biomedical Imaging* (pp. 266–269). IEEE. <https://doi.org/10.1109/isbi.2013.6556463>
- Faul, F., Erdfelder, E., Buchner, A., & Lang, A. G. (2009). Statistical power analyses using G*Power 3.1: Tests for correlation and regression analyses. *Behavior Research Methods*, *41*(4), 1149–1160. <https://doi.org/10.3758/brm.41.4.1149>
- Faul, F., Erdfelder, E., Lang, A. G., & Buchner, A. (2007). G*Power 3: a flexible statistical power analysis program for the social, behavioral, and biomedical sciences. *Behavior Research Methods*, *39*(2), 175–191. <https://doi.org/10.3758/bf03193146>
- Fjell, A. M., McEvoy, L., Holland, D., Dale, A. M., & Walhovd, K. B. (2014). What is normal in normal aging? Effects of aging, amyloid and Alzheimer's disease on the cerebral cortex and the hippocampus. *Progress in Neurobiology*, *117*, 20–40. <https://doi.org/10.1016/j.pneurobio.2014.02.004>
- Gao, Y., Sengupta, A., Li, M., Zu, Z., Rogers, B. P., Anderson, A. W., Ding, Z., & Gore, J. C. (2020). Functional connectivity of white matter as a biomarker of cognitive decline in Alzheimer's disease. *PLoS ONE*, *15*(10), e0240513. <https://doi.org/10.1371/journal.pone.0240513>
- Hoy, A. R., Ly, M., Carlsson, C. M., Okonkwo, O. C., Zetterberg, H., Blennow, K., Sager, M. A., Asthana, S., Johnson, S. C., Alexander, A. L., & Bendlin, B. B. (2017). Microstructural white matter alterations in preclinical Alzheimer's disease detected using free water elimination diffusion tensor imaging. *PLoS ONE*, *12*(3), e0173982. <https://doi.org/10.1371/journal.pone.0173982>
- Hyman, B. T., Phelps, C. H., Beach, T. G., Bigio, E. H., Cairns, N. J., Carrillo, M. C., Dickson, D. W., Duyckaerts, C., Frosch, M. P., Masliah, E., Mirra, S. S., Nelson, P. T., Schneider, J. A., Thal, D. R., Thies, B., Trojanowski, J. Q., Vinters, H. V., & Montine, T. J. (2012). National Institute on Aging-Alzheimer's Association guidelines for the neuropathologic assessment of Alzheimer's disease. *Alzheimers Dement*, *8*(1), 1–13. <https://doi.org/10.1016/j.jalz.2011.10.007>
- Jack, C. R. Jr., Bennett, D. A., Blennow, K., Carrillo, M. C., Dunn, B., Haeberlein, S. B., Holtzman, D. M., Jagust, W., Jessen, F., Karlawish, J., Liu, E., Molinuevo, J. L., Montine, T., Phelps, C., Rankin, K. P., Rowe, C. C., Scheltens, P., Siemers, E., Snyder, H. M., & Sperling, R. (2018). NIA-AA Research Framework: Toward a biological definition of Alzheimer's disease. *Alzheimers Dement*, *14*(4), 535–562. <https://doi.org/10.1016/j.jalz.2018.02.018>
- Kantarci, K., Murray, M. E., Schwarz, C. G., Reid, R. I., Przybelski, S. A., Lesnick, T., Zuk, S. M., Raman, M. R., Senjem, M. L., Gunter, J. L., Boeve, B. F., Knopman, D. S., Parisi, J. E., Petersen, R. C., Jack, C. R. Jr., & Dickson, D. W. (2017). White-matter integrity on DTI and the pathologic staging of Alzheimer's disease. *Neurobiology of Aging*, *56*, 172–179. <https://doi.org/10.1016/j.neurobiolaging.2017.04.024>
- Kumar, A., Sidhu, J., Goyal, A., & Tsao, J. W. (2021). *Alzheimer disease*. StatPearls Publishing LLC.
- Li, J., Fan, Y., Hou, B., Huang, X., Lei, D., Wang, J., Mao, C., Dong, L., Liu, C., Feng, F., Xu, Q., Cui, L., & Gao, J. (2021). A longitudinal observation of brain structure between AD and FTL. *Clinical Neurology and Neurosurgery*, *205*, 106604. <https://doi.org/10.1016/j.clineuro.2021.106604>
- Lu, Y., Li, X., Geng, D., Mei, N., Wu, P. Y., Huang, C. C., Jia, T., Zhao, Y., Wang, D., Xiao, A., & Yin, B. (2020). Cerebral microstructural changes in COVID-19 patients—An MRI-based 3-month follow-up study. *EClinicalMedicine*, *25*, 100484. <https://doi.org/10.1016/j.eclinm.2020.100484>
- Lubben, N., Ensink, E., Coetzee, G. A., & Labrie, V. (2021). The enigma and implications of brain hemispheric asymmetry in neurodegenerative diseases. *Brain Communications*, *3*(3), fcab211. <https://doi.org/10.1093/braincomms/fcab211>
- Minkova, L., Habich, A., Peter, J., Kaller, C. P., Eickhoff, S. B., & Klöppel, S. (2017). Gray matter asymmetries in aging and neurodegeneration: A review and meta-analysis. *Human Brain Mapping*, *38*(12), 5890–5904. <https://doi.org/10.1002/hbm.23772>
- Mito, R., Raffelt, D., Dhollander, T., Vaughan, D. N., Tournier, J. D., Salvado, O., Brodtmann, A., Rowe, C. C., Villemagne, V. L., & Connelly, A. (2018). Fibre-specific white matter reductions in Alzheimer's disease and mild cognitive impairment. *Brain*, *141*(3), 888–902. <https://doi.org/10.1093/brain/awx355>
- Muthen, B. D. K. (1985). A comparison of some methodologies for the factor analysis of non-normal Likert variables. *British Journal of Mathematical and Statistical Psychology*, *18*(38), 171–189. <https://doi.org/10.1111/j.2044-8317.1985.tb00832.x>

- Nir, T. M., Jahanshad, N., Villalon-Reina, J. E., Toga, A. W., Jack, C. R., Weiner, M. W., & Thompson, P. M. (2013). Effectiveness of regional DTI measures in distinguishing Alzheimer's disease, MCI, and normal aging. *NeuroImage: Clinical*, 3, 180–195. <https://doi.org/10.1016/j.nicl.2013.07.006>
- Nir, T. M., Villalon-Reina, J. E., Prasad, G., Jahanshad, N., Joshi, S. H., Toga, A. W., Bernstein, M. A., Jack, C. R. Jr., Weiner, M. W., & Thompson, P. M. (2015). Diffusion weighted imaging-based maximum density path analysis and classification of Alzheimer's disease. *Neurobiology of Aging*, 36(Suppl 1), S132–S140. <https://doi.org/10.1016/j.neurobiolaging.2014.05.037>
- Nishioka, C., Poh, C., & Sun, S. W. (2015). Diffusion tensor imaging reveals visual pathway damage in patients with mild cognitive impairment and Alzheimer's disease. *Journal of Alzheimer's Disease*, 45(1), 97–107. <https://doi.org/10.3233/jad-141239>
- O'Dwyer, L., Lambertson, F., Bokde, A. L., Ewers, M., Faluy, Y. O., Tanner, C., Mazoyer, B., O'Neill, D., Bartley, M., Collins, R., Coughlan, T., Prvulovic, D., & Hampel, H. (2012). Sexual dimorphism in healthy aging and mild cognitive impairment: A DTI study. *PLoS ONE*, 7(7), e37021. <https://doi.org/10.1371/journal.pone.0037021>
- Pereira, J. B., Ossenkoppele, R., Palmqvist, S., Strandberg, T. O., Smith, R., Westman, E., & Hansson, O. (2019). Amyloid and tau accumulate across distinct spatial networks and are differentially associated with brain connectivity. *eLife*, 8, e50830. <https://doi.org/10.7554/eLife.50830>
- Qin, L., Guo, Z., McClure, M. A., & Mu, Q. (2021). White matter changes from mild cognitive impairment to Alzheimer's disease: A meta-analysis. *Acta Neurologica Belgica*, 121(6), 1435–1447. <https://doi.org/10.1007/s13760-020-01322-5>
- Ribeiro, F. S., Teixeira-Santos, A. C., & Leist, A. K. (2022). The prevalence of mild cognitive impairment in Latin America and the Caribbean: A systematic review and meta-analysis. *Aging & Mental Health*, 26(9), 1710–1720. <https://doi.org/10.1080/13607863.2021.2003297>
- Rieckmann, A., Van Dijk, K. R., Sperling, R. A., Johnson, K. A., Buckner, R. L., & Hedden, T. (2016). Accelerated decline in white matter integrity in clinically normal individuals at risk for Alzheimer's disease. *Neurobiology of Aging*, 42, 177–188. <https://doi.org/10.1016/j.neurobiolaging.2016.03.016>
- Sánchez, S. M., Duarte-Abritta, B., Abulafia, C., De Pino, G., Bocaccio, H., Castro, M. N., Sevlever, G. E., Fonzo, G. A., Nemeroff, C. B., Gustafson, D. R., Guinjoan, S. M., & Villarreal, M. F. (2020). White matter fiber density abnormalities in cognitively normal adults at risk for late-onset Alzheimer's disease. *Journal of Psychiatric Research*, 122, 79–87. <https://doi.org/10.1016/j.jpsychires.2019.12.019>
- Schaeffer, M. J., Chan, L., & Barber, P. A. (2021). The neuroimaging of neurodegenerative and vascular disease in the secondary prevention of cognitive decline. *Neural Regeneration Research*, 16(8), 1490–1499. <https://doi.org/10.4103/1673-5374.303011>
- Sepehrband, F., Cabeen, R. P., Choupan, J., Barisano, G., Law, M., & Toga, A. W. (2019). Perivascular space fluid contributes to diffusion tensor imaging changes in white matter. *NeuroImage*, 197, 243–254. <https://doi.org/10.1016/j.neuroimage.2019.04.070>
- Song, S. K., Yoshino, J., Le, T. Q., Lin, S. J., Sun, S. W., Cross, A. H., & Armstrong, R. C. (2005). Demyelination increases radial diffusivity in corpus callosum of mouse brain. *NeuroImage*, 26(1), 132–140. <https://doi.org/10.1016/j.neuroimage.2005.01.028>
- Strain, J. F., Smith, R. X., Beaumont, H., Roe, C. M., Gordon, B. A., Mishra, S., Adeyemo, B., Christensen, J. J., Su, Y., Morris, J. C., Benzinger, T. L. S., & Ances, B. M. (2018). Loss of white matter integrity reflects tau accumulation in Alzheimer disease defined regions. *Neurology*, 91(4), e313–e318. <https://doi.org/10.1212/wnl.0000000000005864>
- Wassenaar, T. M., Yaffe, K., van der Werf, Y. D., & Sexton, C. E. (2018). Associations between modifiable risk factors and white matter of the aging brain: Insights from diffusion tensor imaging studies. *Neurobiology of Aging*, 80, 56–70. <https://doi.org/10.1016/j.neurobiolaging.2018.04.006>
- Weiler, M., de Campos, B. M., Teixeira, C. V. L., Casseb, R. F., Carletti-Cassani, A., Vicentini, J. E., Magalhães, T. N. C., Talib, L. L., Forlenza, O. V., & Balthazar, M. L. F. (2017). Intranetwork and internetwork connectivity in patients with Alzheimer disease and the association with cerebrospinal fluid biomarker levels. *Journal of Psychiatry & Neuroscience*, 42(6), 366–377. <https://doi.org/10.1503/jpn.160180>
- Wen, Q., Mustafi, S. M., Li, J., Risacher, S. L., Tallman, E., Brown, S. A., West, J. D., Harezlak, J., Farlow, M. R., Unverzagt, F. W., Gao, S., Apostolova, L. G., Saykin, A. J., & Wu, Y. C. (2018). White matter alterations in early-stage Alzheimer's disease: A tract-specific study. *Alzheimer's & Dementia*, 11, 576–587. <https://doi.org/10.1016/j.dadm.2019.06.003>
- Wu, Y. C., Field, A. S., Whalen, P. J., & Alexander, A. L. (2011). Age- and gender-related changes in the normal human brain using hybrid diffusion imaging (HYDI). *NeuroImage*, 54(3), 1840–1853. <https://doi.org/10.1016/j.neuroimage.2010.09.067>
- Zhang, B., Xu, Y., Zhu, B., & Kantarci, K. (2014). The role of diffusion tensor imaging in detecting microstructural changes in prodromal Alzheimer's disease. *CNS Neuroscience & Therapeutics*, 20(1), 3–9. <https://doi.org/10.1111/cns.12166>
- Zhuang, L., Sachdev, P. S., Trollor, J. N., Reppermund, S., Kochan, N. A., Brodaty, H., & Wen, W. (2013). Microstructural white matter changes, not hippocampal atrophy, detect early amnesic mild cognitive impairment. *PLoS ONE*, 8(3), e58887. <https://doi.org/10.1371/journal.pone.0058887>

SUPPORTING INFORMATION

Additional supporting information can be found online in the Supporting Information section at the end of this article.

How to cite this article: Xiao, D., Wang, K., Theriault, L., Charbel, E., & Alzheimer's Disease Neuroimaging Initiative (2022). White matter integrity and key structures affected in Alzheimer's disease characterized by diffusion tensor imaging. *European Journal of Neuroscience*, 1–13. <https://doi.org/10.1111/ejn.15815>